

# A Trajectory Based Estimate of the Tropospheric Column Ozone Column Using the Residual Method

M. R. Schoeberl<sup>1</sup>, J. R. Ziemke<sup>2</sup>, B. Bojkov<sup>2,3</sup>, N. Livesey<sup>4</sup>, B. Duncan<sup>2</sup>, S. Strahan<sup>2</sup>, L. Froidevaux<sup>4</sup>, S. Kulawik<sup>4</sup>, P. K. Bhartia<sup>1</sup>, S. Chandra<sup>2</sup>, P. F. Levelt<sup>5</sup>, J. C. Witte<sup>6</sup>, A. M. Thompson<sup>7</sup>, E. Cuevas<sup>8</sup>, A. Redondas<sup>8</sup>, D. W. Tarasick<sup>9</sup>, J. Davies<sup>9</sup>, G. Bodeker<sup>10</sup>, G. Hansen<sup>11</sup>, B. J. Johnson<sup>12</sup>, S. J. Oltmans<sup>12</sup>, H. Vömel<sup>37</sup>, M. Allaart<sup>5</sup>, H. Kelder<sup>5</sup>, M. Newchurch<sup>13</sup>, S. Godin-Beekmann<sup>14</sup>, G. Ancellet<sup>14</sup>, H. Claude<sup>15</sup>, S. B. Andersen<sup>16</sup>, E. Kyrö<sup>17</sup>, M. Parrondos<sup>18</sup>, M. Yela<sup>18</sup>, G. Zablocki<sup>19</sup>, D. Moore<sup>20</sup>, H. Dier<sup>21</sup>, P. von der Gathen<sup>22</sup>, P. Viatte<sup>23</sup>, R. Stübi<sup>23</sup>, B. Calpini<sup>23</sup>, P. Skrivankova<sup>24</sup>, V. Dorokhov<sup>25</sup>, H. de Backer<sup>26</sup>, F. J. Schmidlin<sup>27</sup>, G. Coetzee<sup>28</sup>, M. Fujiwara<sup>29</sup>, V. Thouret<sup>30</sup>, F. Posny<sup>31</sup>, G. Morris<sup>32</sup>, J. Merrill<sup>33</sup>, C. P. Leong<sup>34</sup>, G. Koenig-Langlo<sup>35</sup>, E. Joseph<sup>36</sup>

<sup>1</sup>NASA Goddard Space Flight Center, MD, USA.

<sup>2</sup>University of Maryland Baltimore County (UMBC) Goddard Earth Sciences and Technology (GEST), MD, USA

<sup>3</sup>Also at NASA Goddard Space Flight Center, Greenbelt, MD, USA

<sup>4</sup>NASA Jet Propulsion Laboratory, Pasadena, CA, USA

<sup>5</sup>Royal Netherlands Meteorological Institute, De Bilt, NL

<sup>6</sup>Science Systems and Applications Inc., Lanham, Greenbelt, Maryland, USA

<sup>7</sup>Pennsylvania State, University Park, PA, USA

<sup>8</sup>National Institute of Meteorology, Izana Observatory, Tenerife, SP

<sup>9</sup>Environment Canada, Downsview, Ontario, CA, USA

<sup>10</sup>National Institute of Water and Atmospheric Research (NIWA), Lauder, NZ

<sup>11</sup>Norwegian Institute for Air Research, Tromso, NO

<sup>12</sup>NOAA ESRL/GMD, Boulder, CO, USA

<sup>13</sup>University of Alabama-Huntsville, Atmospheric Science Department, Huntsville, AL, USA

<sup>14</sup>Service d'Aeronomie, CNRS/UPMC, Paris FR

<sup>15</sup>Hohenpeissenberg, German Weather Service, DE

<sup>16</sup>Danish Meteorological Institute, Copenhagen, DK

<sup>17</sup>Finish Meteorlogical Institute/ Arctic Research Center, Sodankyla, FI

<sup>18</sup>Spanish Space Agency, Madrid, SP

<sup>19</sup>National Institute of Meteorology and Hydrology, Legionowo, PL

<sup>20</sup>UKMO, Lerwick, UK

<sup>21</sup>German Weather Service, Lindenberg, DE

<sup>22</sup>AWI, Potsdam, DE

<sup>23</sup>MeteoSwiss, Payerne, CH

<sup>24</sup>Czech Hydrometeorological Institute, Prague, CZ

<sup>25</sup>CAO, Moscow, RU

<sup>26</sup>KMI, Uccle, BE

<sup>27</sup>NASA/GSFC, Wallops Is., Va., USA

<sup>28</sup>South African Weather Service (SAWS), Pretoria, SA

<sup>29</sup>Graduate School of Environmental Earth Science, Hokkaido University, Sapporo, JP

<sup>30</sup>Laboratoire d'Aerologie du CNRS (CNRS/LA), Toulouse, FR

<sup>31</sup>Laboratoire de Physique de l'Atmosphère de la Reunion, La Reunion, FR

<sup>32</sup> Valparaiso University, Valparaiso, IN, USA

<sup>33</sup> University of Rhode Island, Graduate School of Oceanography, Narragansett, RI, USA

<sup>34</sup> Malaysian Meteorological Service (MMS), Jalan Sultan, Selangor, Malaysia

<sup>35</sup> Alfred Wegener Institute (AWI), Bremerhaven, DL

<sup>36</sup> Howard University, Washington D.C., USA

<sup>37</sup> Cooperative Institute for Research in Environmental Sciences, University of Colorado, CO, USA

**Abstract.** We estimate the tropospheric column ozone using a forward trajectory model to increase the horizontal resolution of the Aura Microwave Limb Sounder (MLS) derived stratospheric column ozone (SCO). Subtracting the MLS SCO from Ozone Monitoring Instrument (OMI) column measurements gives the trajectory enhanced tropospheric ozone residual (TTOR). Because of different tropopause definitions, we validate the basic residual technique by computing the 200hPa- to-surface column (200TSC) and comparing it to the same product from ozonesondes and Tropospheric Emission Spectrometer measurements. Comparisons show good agreement in the tropics and reasonable agreement at middle latitudes, but there is a persistent low bias in the TTOR that may be due to a slight high bias in MLS SCO. With the improved SCO resolution, we note a strong correlation of extra-tropical TCO anomalies with probable troposphere-stratosphere exchange events or folds. The folds can be identified by their co-location with strong horizontal tropopause gradients. TTOR anomalies due to folds may be mistaken for pollution events since folds often occur in the Atlantic and Pacific pollution corridors. We also compare the 200TSC with Global Modeling Initiative (GMI) chemical model estimates of the same quantity. While the tropical comparisons are good, we note that GMI variations in 200TSC at middle latitudes are much smaller than seen in the TTOR.

## 1. Introduction

The tropospheric column ozone residual (TOR) method estimates the tropospheric column ozone (TCO) by subtracting measurements of stratospheric column ozone (SCO) from total column ozone. The tropospheric ozone column rarely exceeds 80 DU and thus is always a smaller component of the total ozone column (~ 250 - 500 DU). Total ozone column has been accurately measured by the Total Ozone Mapping Spectrometer (TOMS) instrument series starting in late 1978 and most recently the Dutch-Finnish Ozone Monitoring Instrument (OMI) [Levelt *et al.*,

2006] on Aura. Although direct measurement of TCO using UV instruments is possible [e.g. Liu et al., 2006], we focus on the residual technique in this paper. The key to producing the TCO is an accurate estimation of the larger stratospheric column ozone (SCO). Various instruments have been used to derive the SCO including Stratospheric Aerosol and Gas Experiment II [Fishman and Larsen, 1987, and Fishman et al., 1990], Upper Atmosphere Research Satellite (UARS) Microwave Limb Sounder (MLS) [Chandra et al., 2003] and Aura's Earth Observing System MLS [Ziemke et al, 2006, hereafter Z06]. Up until the launch of Aura and ENVISAT, near simultaneous SCO and total column ozone amounts were not available. A brief review of TOR techniques is given in Z06 and is not repeated here.

The Aura MLS instrument [Waters et al., 2006] can be used to estimate the SCO as in Z06. One advantage of the Aura MLS over the previous UARS MLS instrument is that Aura MLS was designed to retrieve ozone in the lower stratosphere and upper troposphere (UTLS). The second advantage is that because Aura is in a sun-synchronous orbit, Aura MLS instrument can produce near global maps of SCO on a daily basis. The OMI and MLS instruments onboard the Aura spacecraft have been providing global measurements of total column ozone and SCO soon after the launch of Aura on July 15, 2004 [Schoeberl et al., 2006]. This has enabled near global estimates of TCO on almost a day-to-day basis from late September 2004 to present.

In Z06, Aura MLS SCO and OMI TCO data were used to produce a monthly mean and daily TOR. However, with only  $\sim$ 14.6 orbits a day, the MLS ascending node (daytime) measurements of SCO provide only a low horizontal resolution mapped product ( $\sim$ 24.7° longitude by  $\sim$ 2° latitude). The interpolation of MLS data onto the OMI grid to generate the TOR, implicitly forces smaller scale variability seen in the OMI total column ozone to be part of the tropospheric column. This assumption probably does not strongly affect the computation of the monthly mean TOR because the smaller scale variability will average out in a month. Indeed, Z06 showed that monthly mean sonde profiles were consistent with TOR estimates from ozonesondes. However, to produce a reasonable daily product, the approach used by Z06 has to be modified to account for SCO spatial variability.

In this study, we use forward trajectory calculations to boost the horizontal resolution of the SCO, and this allows us to generate an improved daily TOR. In the next section, we describe the data

and method. We validate our results with daily ozonesondes. We also compare the data with Tropospheric Emission Spectrometer (TES) [Beer, 2006] direct estimates of the ozone column. We show some examples of tropopause folds that are clearly present in the observations and how our estimates of the TCO compare with NASA Global Modeling Initiative (GMI) estimates of the column (see Z06).

## 2. Overview of Method

OMI is a nadir-scanning instrument that detects backscattered solar radiance to measure column ozone. OMI pixels have a nadir resolution of  $13\text{ km} \times 24\text{ km}$  [Levelt *et al.*, 2006]. Total ozone from OMI is derived using the TOMS version 8 algorithm [Bhartia, 2007].

The Aura MLS instrument measures vertical profiles of mesospheric, stratospheric, and upper tropospheric temperature, ozone and other constituents from limb scans. The MLS profile measurements are taken about 7 minutes before OMI views the same location during daytime orbital tracks. Details regarding the instrument including spectrometers, spectral channels, calibration, and other topics are discussed by Waters *et al.* [2006]. Froidevaux *et al.* [2006] provide early validation results on the Aura MLS algorithm version 1.5 measurements of ozone and other constituents; version 1.5 is used here.

About two and a half years of ozone data have been archived as level 2GP for MLS and level 2 gridded (L2G), and level-3 (L3) for OMI beginning in September 2004. Z06 use the OMI L3 and MLS L2 (ascending node only) data to produce maps of SCO and TOR. In Z06, SCO is generated by interpolating between MLS measurement points that are  $\sim 25^\circ$  in longitude apart. This approach assigns the smaller scale variability of the SCO to the TCO. Increasing the resolution of the SCO map would improve the TCO estimate. There are at least two approaches to increasing the SCO resolution: (1) MLS data can be trajectory mapped [Morris *et al.*, 2000] to form a higher resolution field. (2) MLS data can be assimilated in a 3D chemical model (see Stajner *et al.*, this issue, 2007). In this study we take the former approach while acknowledging that full 3D chemical assimilation is probably the ultimate solution since modern assimilation techniques better handle instrumental and meteorological measurement uncertainties.

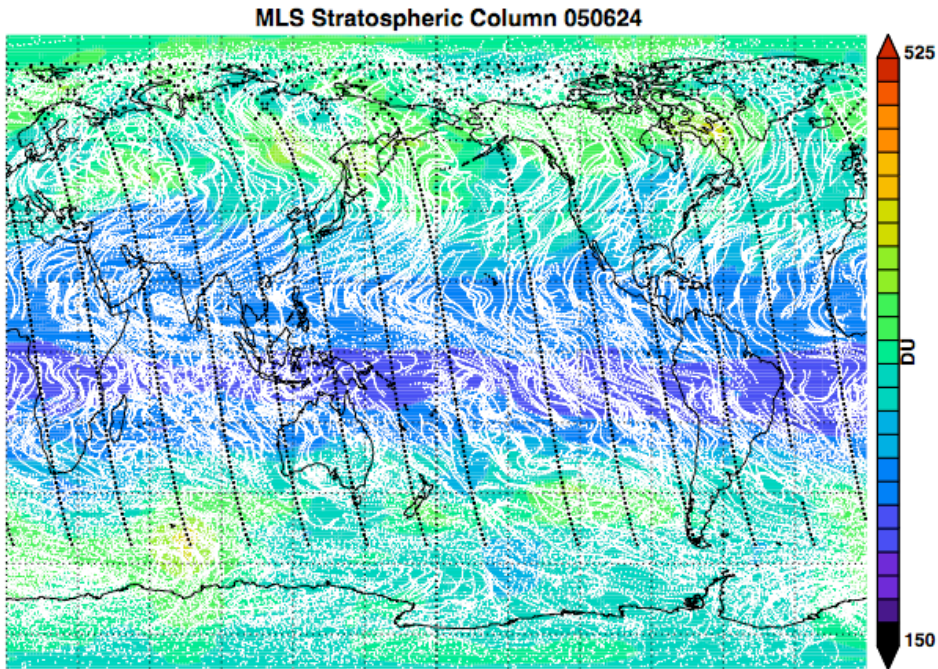
The trajectory mapping approach is to simply move the measurement made at one time to another time using the trajectory model and assimilated meteorological data. We used only forward mapping here. (*Morris et al.* [2000] used both forward and backward mapping.) MLS ozone profiles precision percentage uncertainty increases moving from the stratosphere downward into the upper troposphere. Measurements below about 215 hPa (near the mid-latitude tropopause) are probably not accurate enough for our purposes. Since we wish to avoid data from below 215 hPa produced by backward trajectories ascending into the mid-latitude stratosphere we restrict ourselves to forward trajectory mapping. The ascent of air from below 215 hPa into the stratosphere is not as much of a concern in the tropics because the ascent is slow and the 215 hPa level is well below the tropopause.

The six days of forward trajectories accumulating measurements from both day and night MLS observations are accumulated for each analysis day (target day). Our experience with trajectory calculations at these altitudes suggests that six days is the practical time limit for such mapping due to the accumulation of errors associated with the meteorological fields [*Schoeberl and Sparling*, 1995]. For the target day, only the ascending node (daytime) MLS data are used because those data correspond to OMI measurements taken on the same day. The meteorological fields used to drive the trajectory model are the GEOS-4 winds and temperatures [*Bloom et al.*, 2005]. Experiments with the technique show that we only need to trajectory map data below 30 km and we can use the Z06 spatial interpolation approach above 30 km.

The procedure is as follows: First, the MLS measurements are screened using the recommended quality flags then the data are interpolated along the MLS track to fill in any missing values. Using the trajectory code, up to six days of measurements points between 215 hPa and 10 hPa are moved forward to a target time. If a trajectory descends below 215 hPa it is removed. At the target time, the MLS ozone data are interpolated onto a map at the GEOS-4 resolution ,  $1^{\circ} \times 1.25^{\circ}$  (latitude, longitude) at the MLS L2 pressure levels .

Figure 1 (top) shows the trajectory locations for points accumulated over the last six days and the actual measurements points for MLS on June 24, 2005 on the 100hPa surface. It is evident that

the forward trajectory mapping significantly increases the amount of data that can be used in generating the SCO map. Fig. 1 (middle) also shows that the increase in data through the forward trajectory system does not produce large scale changes in the SCO, but it does produce subtle changes in the smaller scale features. One additional advantage of the trajectory scheme is that if the MLS instrument is not taking data we can use the data from previous days to generate the SCO.



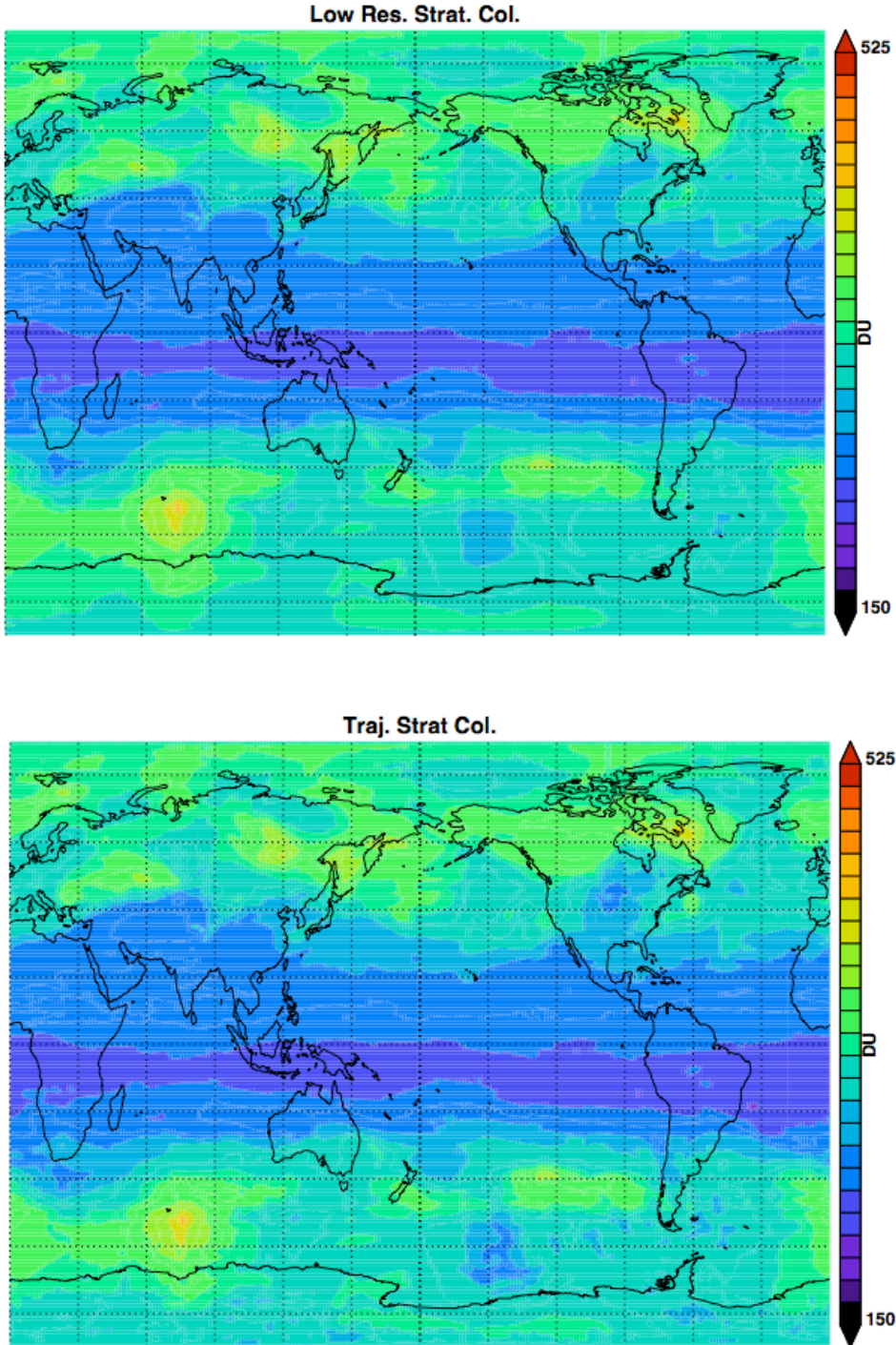


Figure 1. Low resolution tropospheric ozone with MLS measurement points on the target day (black) and forward trajectory points (white) from MLS measurements using the last 6 days of data (upper figure). The middle figure is the same as upper without measurement points. In the upper and middle figures only MLS data from the black measurement points are used. The bottom figure shows the high resolution stratospheric column using all the points shown in the top figure.

After generating the SCO, the OMI total column (OMI-TOMS, from the OMI Algorithm Theoretical Basis Document (ATBD), [http://toms.gsfc.nasa.gov/version8/v8toms\\_atbd.pdf](http://toms.gsfc.nasa.gov/version8/v8toms_atbd.pdf)) measurements are screened via the recommended L2 data quality flags. We use OMI L2G data interpolated to the SCO (GEOS-4) grid. Total ozone data are further screened using the reflectivity – scenes with reflectivity greater than 0.6 are considered cloudy and are not used (1.0 reflectivity is fully cloud covered); Z06 screened data based on 0.3 reflectivity but in our comparisons below the Z06 product is screened for 0.6. In fully cloudy cases, the ozone algorithm uses climatological tropospheric ozone, but even with 0.6 reflectivity, some residual information on the tropospheric ozone is in the data.

Finally, to compute the TOR the tropopause pressure is required. For this study we use the following algorithm for the tropopause: the tropopause is the lowest of the following, the |3.5| PVU surface, the  $< 2 \text{ K-km}^{-1}$  surface (or approximately World Meteorological Organization lapse rate tropopause), the cold point tropopause, the 380K surface. Generally, the PV tropopause is the lower than the lapse-rate tropopause except in the tropics [Schoeberl, 2004; Stajner *et al.*, this issue]. In the tropics, the lapse-rate and cold point tropopause coincide and are rarely above 380K. Choosing the lowest tropopause from the ensemble avoids the complexity that arises when there is a double tropopause [Randel *et al.*, 2007]. Z06 uses the lapse-rate tropopause from NCEP analyses. The different tropopause definitions between analyses creates biases between various computations of the TOR. In the validation section below we use a 200 hPa-to-surface column (200TSC) which removes tropopause pressure level produced biases.

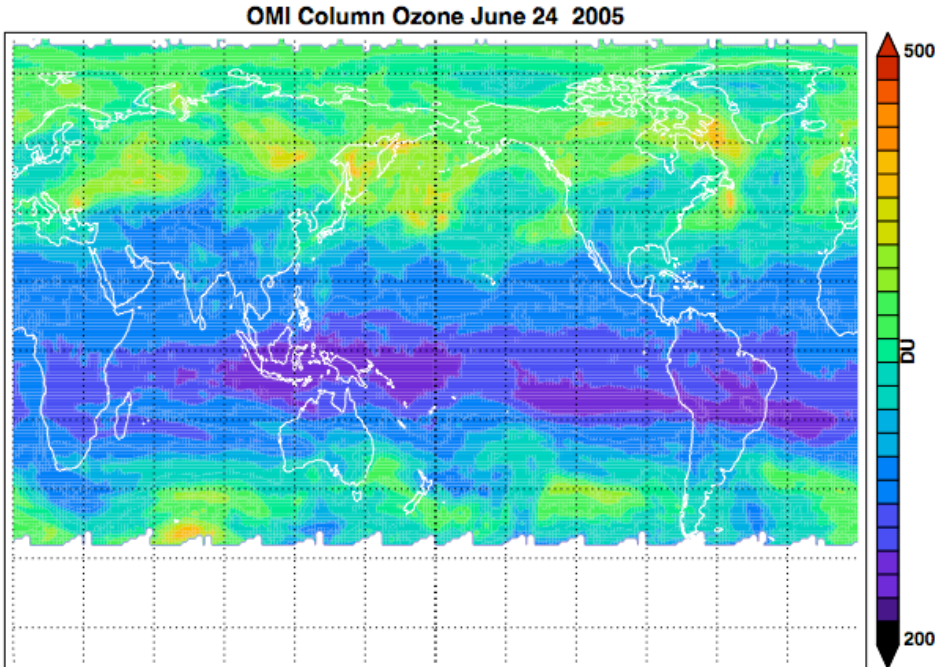
We generate the TOR by subtraction of the SCO from the OMI total ozone column. The OMI and MLS data are not synoptic, that is, the measurement times vary with global location. To generate asynoptic SCO to match the OMI data, the MLS data are forward trajectory transported to the asynoptic times of the OMI data. The tropopause pressure is also time interpolated from the four GEOS-4 synoptic times to the asynoptic OMI TCO. Although this is a much more complicated scheme than simply assuming (as in Z06 and previous studies) that the OMI and MLS fields are synoptic (or time simultaneous), we find that if the asynoptic nature of the data are not considered, tropopause fold anomalies can be significantly overestimated or underestimated. Finally, during the course of our computations we generate a quality flag which

indicates points with high reflectivity, anomalous ozone, low tropopause, L2 flags or other problems. All of the validation calculations discussed below are made with high quality data (no flags).

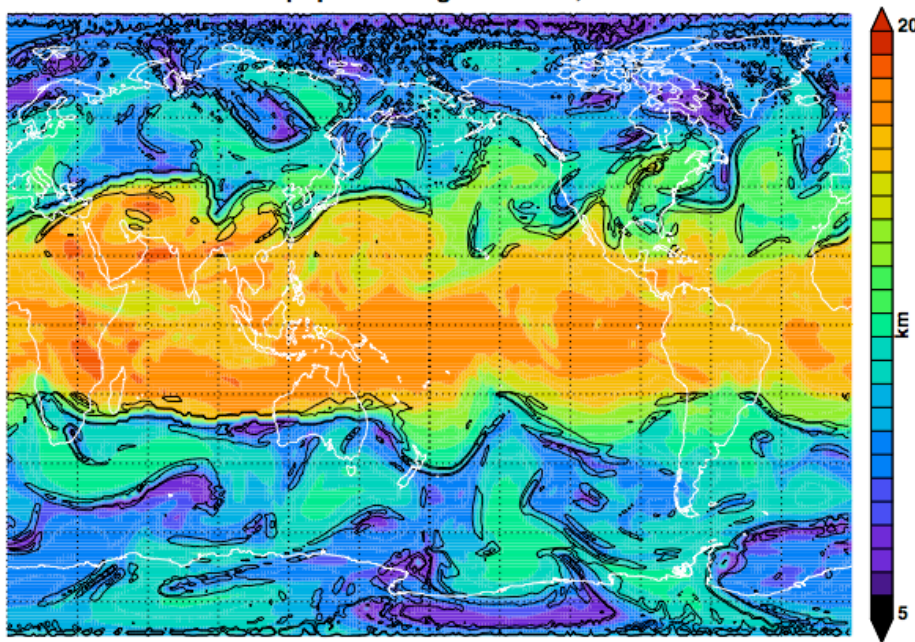
Between any two pressure levels the ozone column in Dobson Units (DU) is

$$ColO_3 = 0.7889 \int_{p_{top}}^{p_{bottom}} \mu dp \quad (1)$$

[Dessler, 2005] where  $\mu$  is ozone volume mixing ratio in units ppbv and  $p$  is pressure ( $p_{top}$  is the lower pressure) in hPa. If we know both the tropopause and surface pressure, we can compute the tropospheric average mixing ratio (TAMR) that would generate the TOR. The principal advantage of the TAMR is that surface pressure changes due to weather or topography that influence the column are removed.



Tropopause Height June 24, 2005



Tropospheric Ozone Column June 24 2005

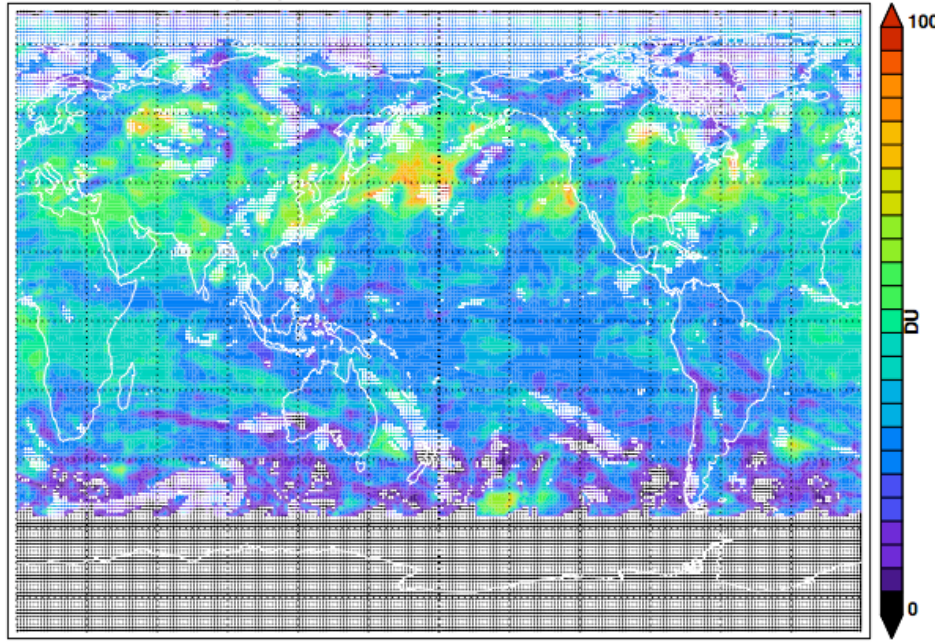


Figure 2. Top, the OMI column ozone field in DU for June 24, 2005 (050624). Middle, the tropopause height in km, black contours show the amplitude of the tropopause gradient. Bottom, the tropospheric ozone residual in DU; crosses indicate points where the quality flag indicates issues with the calculation such as no column measurement, low tropopause or high reflectivity.

Figure 2 shows an example of the fields that are combined with the SCO to generate the TO. The top figure shows the OMI column. We focus our attention on the region of high tropospheric ozone off the east coast of North America. The tropopause height plot (middle, Fig. 2) shows us that there is a strong east-west gradient in that region which is one of the characteristics of a tropopause folding event. The magnitude of the tropopause gradient is contoured in black (units are unimportant). Elsewhere on the map high OMI column amounts are often co-located with the strong east-west tropopause gradients. The TOR also shows high values on the cyclonic side of the jet expected with a stratosphere-troposphere exchange event. This gives us confidence that the TOR captures at least some of the daily variability. *Stajner et al.* (this issue) also note high tropospheric column events on the cyclonic side of the jet in their assimilated tropospheric column. The tropopause ozone gradient is a key factor in interpreting daily results. High, localized TCO events off the east coast of the United States or China that might appear to be pollution events are often folds. In the rest of this paper we refer to TOR products produced using the trajectory method of estimating SCO as trajectory enhanced tropospheric ozone residual (TTOR).

### 3. Validation of OMI/MLS Tropospheric and Stratospheric Ozone Measurements.

MLS ozone validation is discussed by *Froidevaux et al.* [2006]. The V1.5 MLS ozone profiles evaluated for 0.46-215 hPa tend to be within about 1 percent of column amounts calculated from SAGE II, but MLS tends to overestimate ozone in the very lower part of the stratosphere by up to 20% compared to SAGE II and POAM data. The newest version of the MLS algorithm, V2.2, show improvements in lower stratospheric ozone retrievals, *Froidevaux et al.* [2007], but too little V2.2 MLS data has been processed using the newest algorithm to use it here.

OMI total ozone measurements have been extensively validated with both ground-based Brewer and Dobson data, Earth Probe (EP) TOMS data, and Solar Backscatter Ultraviolet (SBUV/2) data. Comparisons between OMI and ground based total column ozone measurements indicates that OMI column ozone is within ~1% of the ground based measurements [*McPeters et al.*, 2007]. To summarize, the MLS SCO may be slightly high biased by a few DU, and if the OMI column has almost no bias, the TTOR will be low biased.

### **3.1 Sonde validation of the 200hPa to surface column**

Z06 discussed comparisons of their TOR product with ozonesonde estimates of the tropospheric column. They found poor agreement on a day-to-day basis but good agreement if the data were averaged into monthly means. A possible explanation for this is that the synoptic product generated by the simple subtraction of MLS SCO from OMI total column ozone cannot account for the dynamic variation of the TCO at extra-tropical latitudes. A monthly mean comparison would show better agreement since folds would average out. Our asynoptic TTOR should show some improvements over Z06.

As discussed above, we focus on the 200TSC to remove issues with the definition of the tropopause. This approach tests the concept of the residual technique itself and separates tropopause issues from the ozone data sets. For the comparison, ozone profiles from over 6,360 tropical and mid-latitude ozonesondes have been used to compute the 200TSC. We use the Southern Hemisphere ADDitional Ozonesondes (SHADOZ) [*Thompson et al.*, 2003] collection, the European Space Agency Envisat Cal/Val collection, the WMO GAW collection and the IONS (INTEX Ozonesonde Network Study) collection [*Thompson et al.*, 2007]. The SHADOZ, GAW and Envisat sonde data base covers late 2004 through 2006; IONS covers late February 2006-September 2006. We compute the 200TSC using the OMI-MLS methods described above and interpolate the result (and the quality flags) to the sonde points; the sonde data have also been screened to within six hours of the Aura overpass times

#### **3.1.2 SHADOZ tropical ozonesondes**

In the mid-latitudes, the tropospheric ozone amounts vary rapidly from day to day and from season to season. By comparison the tropical regions show relatively little rapid temporal variability. Thus there is no need to provide a seasonal analysis as done in the next section.

SHADOZ data are used for our tropical comparisons.

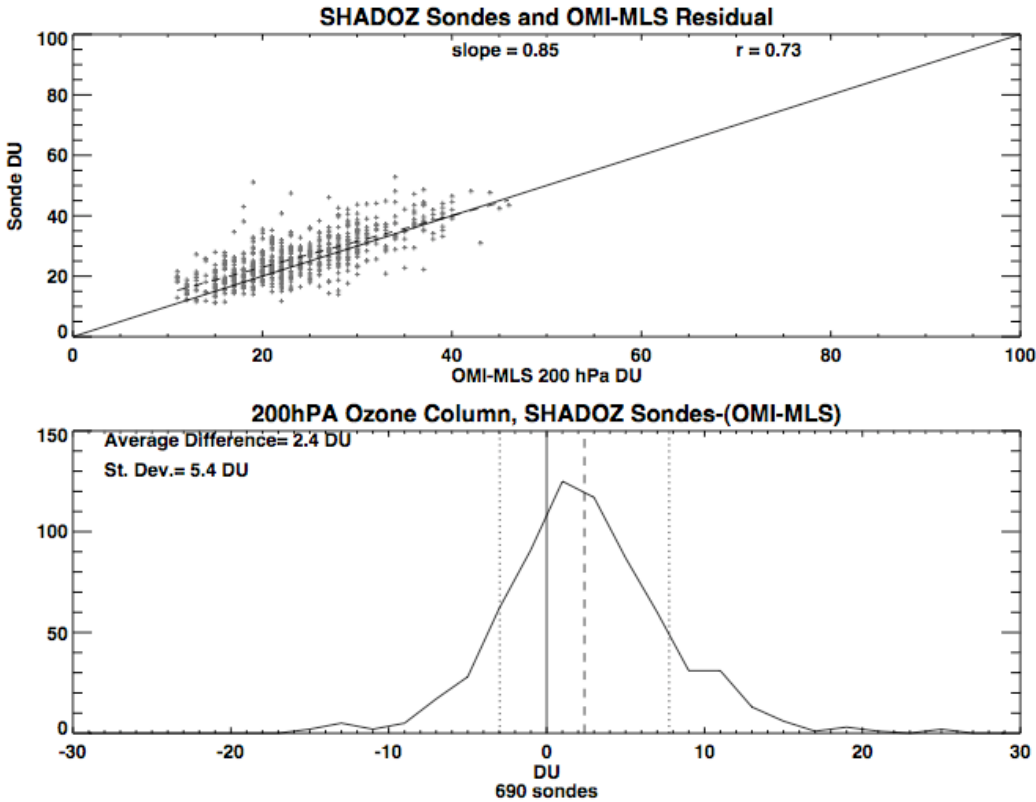
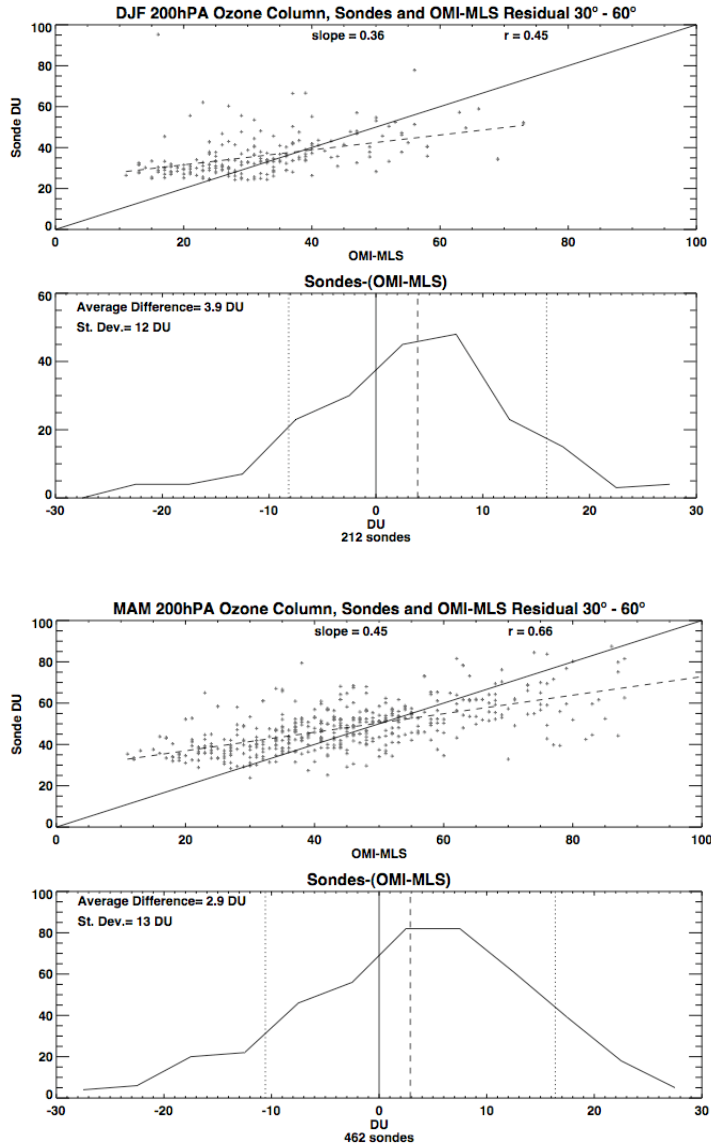


Figure 3. Comparison of ozonesondes 200TSC and the our 200TSC estimate. Upper figure shows the data points, the slope of the data (dashed line) and the correlation coefficient ( $r$ ). The one-to-one line is the solid line. The lower figure shows a PDF of the difference between the sonde 200TSC with the mean and standard deviation (dashed and dotted, respectively).

Figure 3 compares 690 ozonesonde estimates of the TTOR 200TSC over the Aura period. The comparison shows a correlation of 0.73 and a data slope of 0.85. The column offset is 2.4 DU with the ozonesonde profiles having a slightly higher column. This result would be consistent with a slightly high SCO derived from MLS measurements. The standard deviation of ~5 DU in this case represents the combined errors of the trajectory model, measurement error from both MLS and OMI as well as sonde error and thus probably represents the total uncertainty of the measurement.

### 3.1.2 Comparison with mid-latitude ozonesondes by season

In Fig. 4 we show the comparisons at mid-latitudes by season. There are few ozonesondes in the extra-tropical Southern Hemisphere so we restrict our analysis to the extra-tropical Northern Hemisphere.



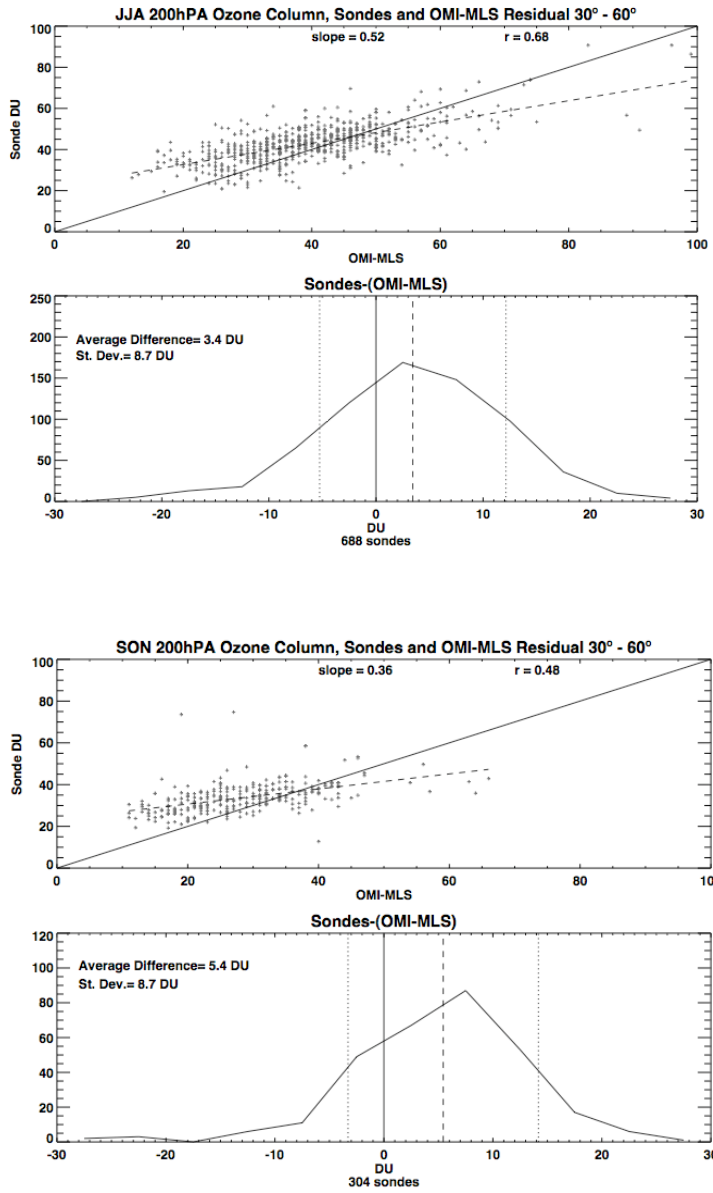


Figure 4 As in Figure 3, except mid-latitude ( $30^{\circ}$ - $60^{\circ}$ N) sonde 200TSC and OMI-MLS 200TSC comparisons for four seasonal periods indicated by the month grouping.

As was seen in the tropics, there is a persistent offset between our OMI-MLS 200TSC and the sonde 200TSC of about 3-5 DU depending on season. The correlation of the sonde and OMI-MLS data are weaker in fall and winter. The ozonesondes generally show less dynamic range than the residual product suggesting that the TTOR is influenced by lower stratospheric ozone since the tropopause is much lower in the middle latitudes. It is important to recognize that MLS

vertical resolution is 2-3 km so that when there is a sharp ozone gradient at the tropopause – as occurs during winter - MLS may incorrectly estimate the SCO. This would give the TTOR greater range than the ozonesondes TOR which is a more precise measure the tropospheric column.

The *Froidevaux et al. [2006]* preliminary validation of MLS V1.5 ozone shows that MLS lower stratospheric ozone is slightly high biased to SAGE II and POAM. A 20% error in typical mid-latitude UTLS ozone profile would produce an SCO increase of ~2-8 DU (depending on the profile) leading to a low bias in the TTOR of about the same amount as is seen above. J. Ziemke [personal communication, 2007] has compared OMI SCO using cloud slicing with MLS SCO and do find that MLS is high biased by 2-3 DU consistent with our results.

The figures also show that the TTOR-sonde difference standard deviation at mid-latitudes is much larger than in the tropics. The greater fluctuation in the TTOR is due to greater fluctuations in the mid-latitude SCO. Nonetheless, although the mid-latitude correlation with sonde data are not as good as in the tropics, the daily TOR product does appear to provide a reasonable assessment of the tropospheric ozone column.

We have also correlated the TTOR with surface station ozone measurements and find only a very weak correlation of 0.12. It is not surprising that the TTOR is not very sensitive to surface values because OMI has low sensitivity to surface ozone due to strong Rayleigh scattering, and surface ozone variability tends to have a smaller spatial scale than the OMI pixel size (13x24 km at nadir).

### **3.2 Comparisons with tropical TES observations**

The Tropospheric Emission Spectrometer (TES) is an infrared Fourier transform spectrometer on Aura [*Beer, 2006*]. TES's high spectral resolution allows direct measurements of the tropospheric ozone. The TES ozone product and sonde validation are described by *Worden et al. [2007]* and *Osterman et al., [2007]*. TES (like OMI) is not very sensitive to ozone at the surface because of lack of temperature contrast between the surface and the lowest atmospheric layer.

Nonetheless, TES measurements should provide a reasonable estimate of the TCO for comparison. As with the sonde comparison we compute the TES 200TSC and interpolate our 200TSC to the TES locations. We use TES data taken from October 1, 2004 through September 20, 2006. TES tropospheric columns were created by integrating the TES reported profile up to 200 hPa. The error for the column can be calculated using the reported profile error covariance, as discussed in *Kulawik et al.*, [2006]. Figure 5 shows the comparison with TES tropical data using ~100,000 points. Comparisons are not screened to local daylight so this group also includes TES measurements at night; in the tropics where ozone varies slowly, the day-night distinction is probably unimportant. Values are cut off at 5 DU for both data sets – it is unlikely that TCO values can ever be that low.

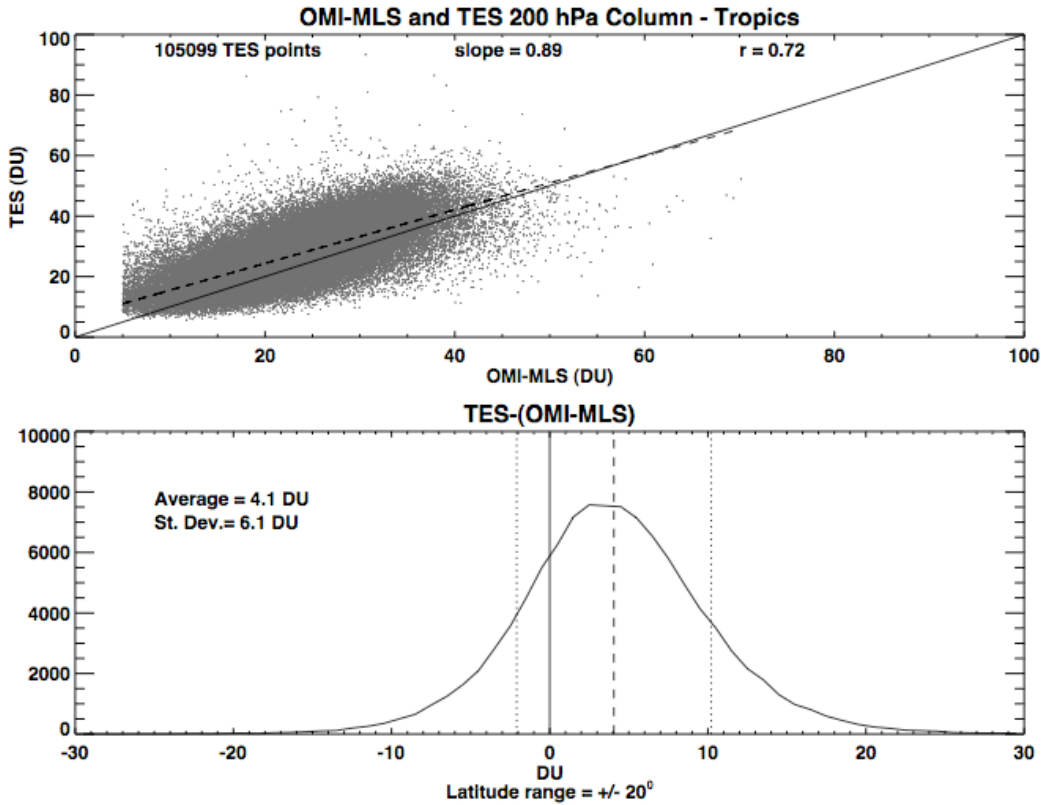
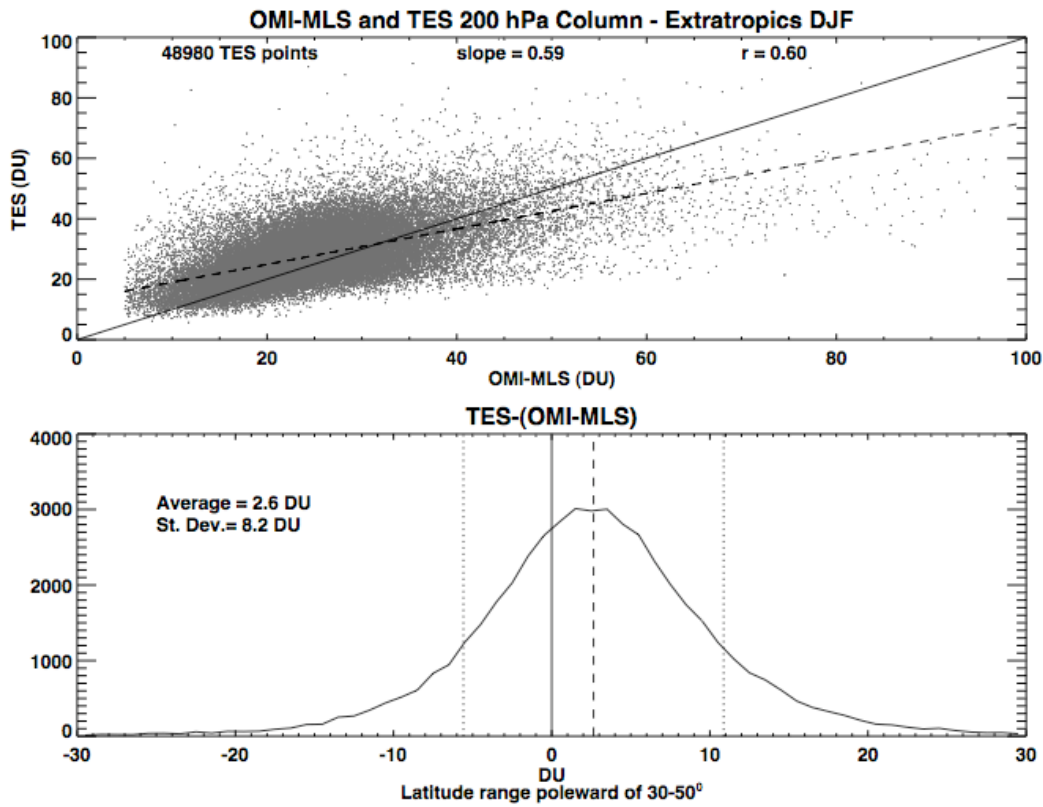


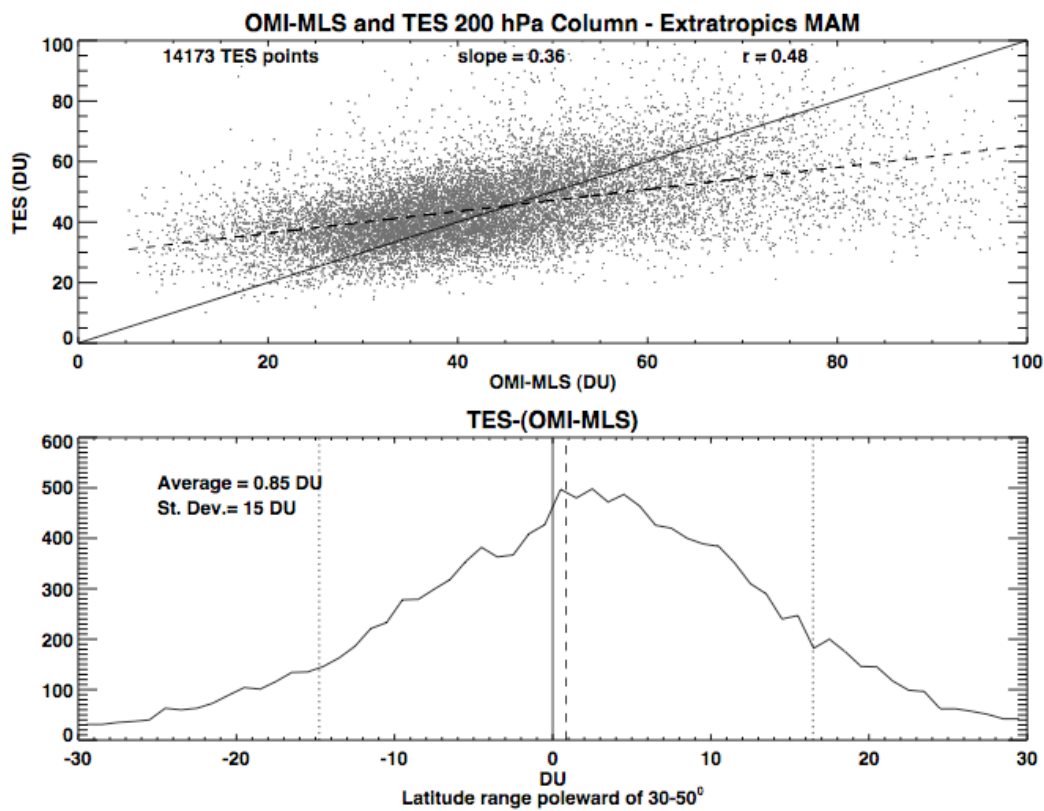
Figure 5. As with Figure 3 except comparisons with TES measurements

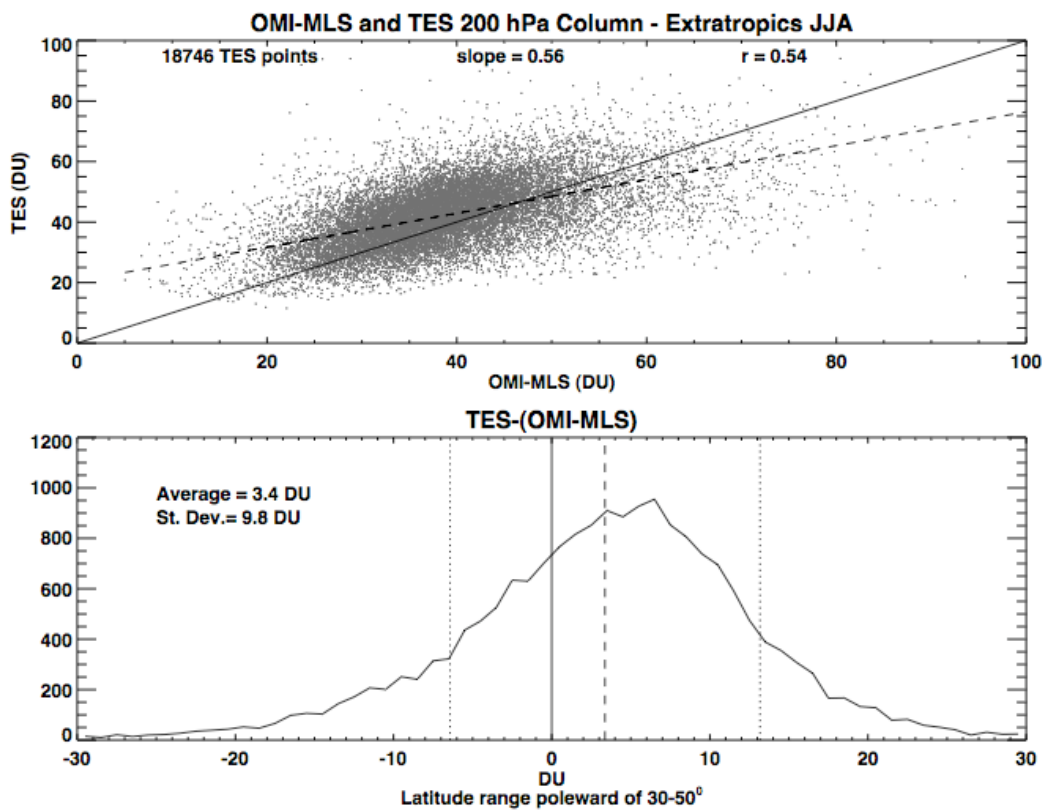
In the tropical regions, the TES and TTOR are in good agreement and correlate well. We note a high bias of about 4.1 DU for TES with a standard deviation of 6.1 DU. *Osterman et al.* [2007]

found TES high biased by about 3.6 DU compared to near coincident ozonesondes on a global average with a standard deviation of 6.8 DU. *Kulawik et al.* [2007] found that TES total ozone column was high biased with respect to OMI column (see their Fig. 8, ~12.5 DU). Our results are generally consistent with *Osterman's et al.* (*op cit*) and *Kulawik's et al.* (*op cit.*) findings. The Gaussian structure of the difference PDF suggests that the differences between TTOR are due to random error.

### 3.3 Seasonal extratropical comparisons with the TES data







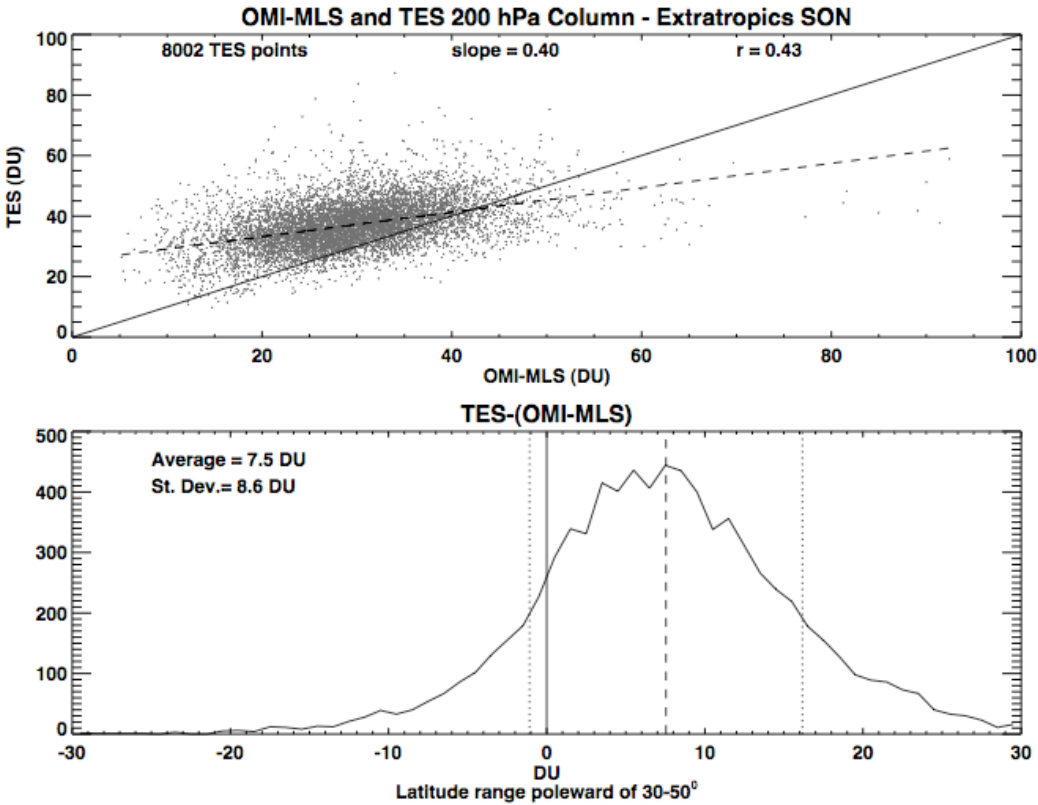


Figure 6. Same as Figure 4 except comparing TES 200 hPa extra-tropical column ( $30^{\circ}$ - $50^{\circ}$  N) with OMI-MLS 200 hPa column.

Figure 6 shows the comparison of the extra-tropical data ( $30^{\circ}$ - $50^{\circ}$ N). The correlation between the data sets is not as high in the extra-tropics (0.43-0.54) as we saw in the tropics (0.6). The biases vary between 0.8 and 7 DU with larger standard deviations than in the tropics. As with our sonde comparison, TES dynamical range is smaller than the TTOR.

### 3.4 Summary of Validation Results

Table 1 summarizes the bias and standard deviations for both the ozonesondes and TES. There is very good agreement in the tropics between the TTOR and the ozonesonde and TES data sets. Outside the tropics there is a wider range in the TTOR 200TSC than seen in TES or sonde 200TSC. The best extra-tropical agreement is in summer when the extra-tropical tropopause is

highest – in other words, when extra-tropical tropopause is elevated like the tropical tropopause. These results suggest that the TTOR is less reliable under low tropopause conditions – when ozone levels are high in the 100-200 hPa UTLS region.

There is a persistent offset between the TTOR and TES or ozonesondes. The TTOR is low biased which could arise either from a high bias in the MLS SCO or a low bias with the OMI ozone column. *McPeters et al.* [2007, this issue] comparison of OMI column ozone with ground stations show no persistent bias suggesting that the problem lies with the MLS SCO. J. Ziemke [personal communication, 2007] has found that the OMI SCO obtained by cloud slicing is consistently lower than the MLS SCO by several DU. *Froidevaux et al.* [2006] also show a high bias in the 100-200 hPa region which could create an SCO column bias.

Table 1. Summary of 200TSC validation results. Biases are positive when OMI-MLS is low compared to the other data set.

Comparison		Tropics	NH Extratropics			
			DJF	MAM	JJA	SON
Ozonesonde	Biases (DU)	2.4	3.9	2.9	3.4	5.4
	Standard Deviation	5.4	12	13	8.7	8.7
	Correlation Coef.	0.73	0.45	0.66	0.68	0.48
TES	Biases	4.1	2.6	0.85	3.4	7.5
	Standard Deviation	6.1	8.2	15	9.8	8.6
	Correlation Coef.	0.72	0.6	0.48	0.54	0.43

#### 4. Daily and Monthly Maps of Tropospheric Average Mixing Ratio

##### 4.1 Daily values

As mentioned above the mid-latitude TOR values are strongly affected by high levels of ozone in the UTLS as occurs with stratosphere-troposphere exchange (STE) processes. This is illustrated in Fig. 7 which shows TAMR for a sequence of four days from May 20-23, 2006.

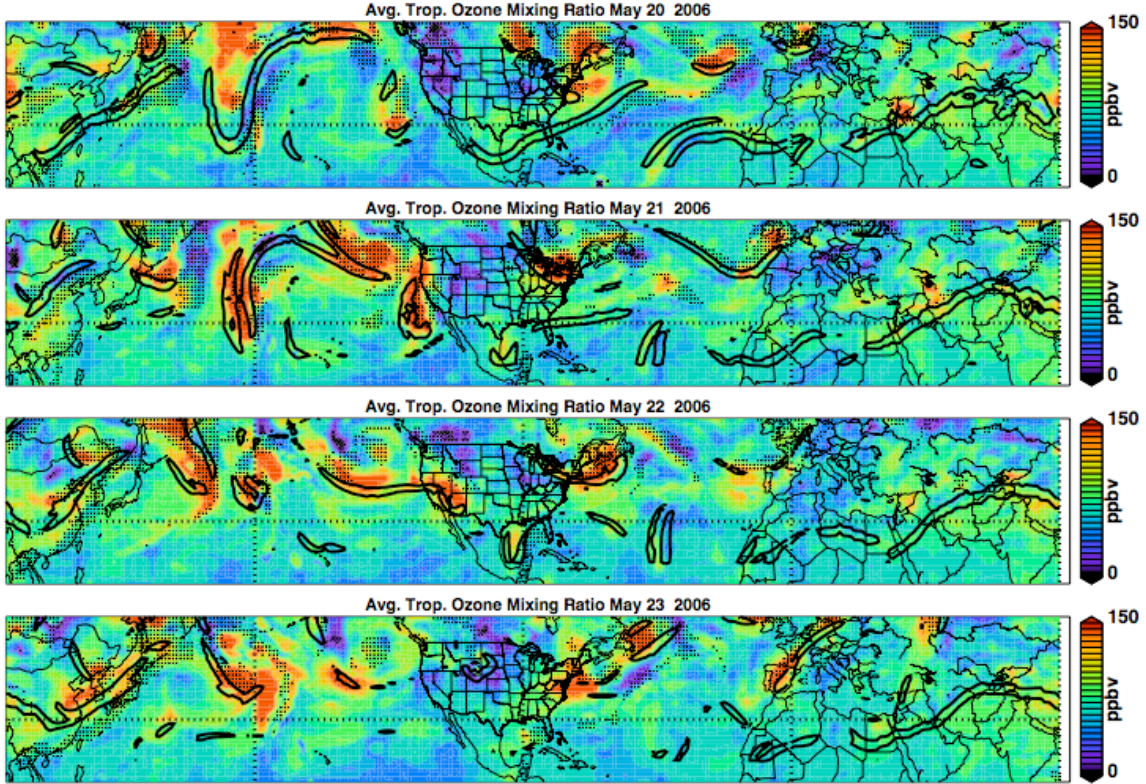


Figure 7. Tropospheric averaged mixing ratio (TAMR) for the sequence May 20-23, 2006. Black contours surround regions where there is a maximum in the tropopause spatial gradient – an indicator of fold locations. Small black dots indicate regions where the data are of questionable quality (i.e. high reflectivity, low tropopause, etc.)

The figure shows that the strong gradients in the tropopause are frequently co-located with the TAMR maxima suggesting that the TOR is strongly influenced by upper tropospheric folding processes [e.g., *de Laat et al.*, 2005 and references therein]. For example, the mid-Pacific maximum on May 21 are clearly due to a folding event. Simultaneously, a folding event is occurring off the east coast of the United States. Folds occur along jet axes and by collocating TAMR enhancements with sharp tropopause gradients we estimate that at least 15% or more of

the monthly mean TOR off the east coast of the United States and East Asia can be attributed to folding events.

#### 4.2 Annual mean values

Folds are highly mobile events and tend to average out of monthly and annual mean data. Figure 8 shows the TOR and TAMR for 2005 and 2006.

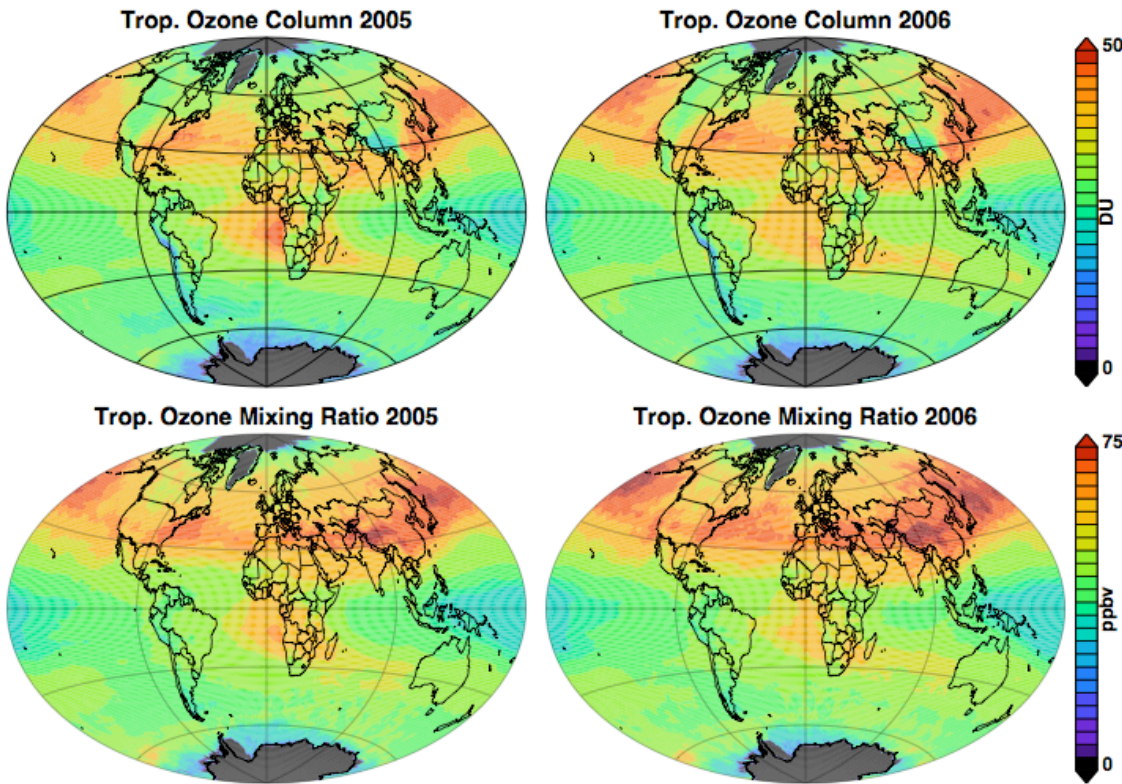


Figure 8. Annual mean maps of TTOR and tropospheric average mixing ratio (TAMR) for 2005 and 2006.

Values are reported on this map if ten days of high quality data can be used for a pixel. Both maps show the characteristics described by Z06 including high values of the Eastern U. S., high values covering Europe, especially the Mediterranean [Lelieveld *et al.*, 2002] to East Asia extending into the Pacific to the West Coast of the U.S. We also note the very low values over

the tropical east Pacific region [Kley, et al., 1996, Martin et al., 2002]. Note the decrease in DU values in the presence of high topography near continental edges or in mountain ranges (top, Fig. 8). This decrease is not present in the mixing ratio plots (bottom, Fig. 8). The decrease is due the change in surface pressure where the topography is high so the total column is smaller (see Eq. 1). This pressure column effect has less impact on the average mixing ratio.

Aside from the similarity between years, there is visible interannual variability. For example, the high ozone features in the South Atlantic and Africa [see for example, Edwards, et al., 2003, , Moxim and Levy, 2000, Marufu et al., 2000, Thompson et al., 1996, Fishman and Larsen, 1987] are more extensive in 2005 than in 2006. Monthly mean data are not shown here but can be downloaded [ftp://hyperion.gsfc.nasa.gov/pub/aura/tropo3/tropo3\\_YYMM.pdf](ftp://hyperion.gsfc.nasa.gov/pub/aura/tropo3/tropo3_YYMM.pdf) where MM indicates the month number (e.g. 06) and YY the year number (e.g. 05).

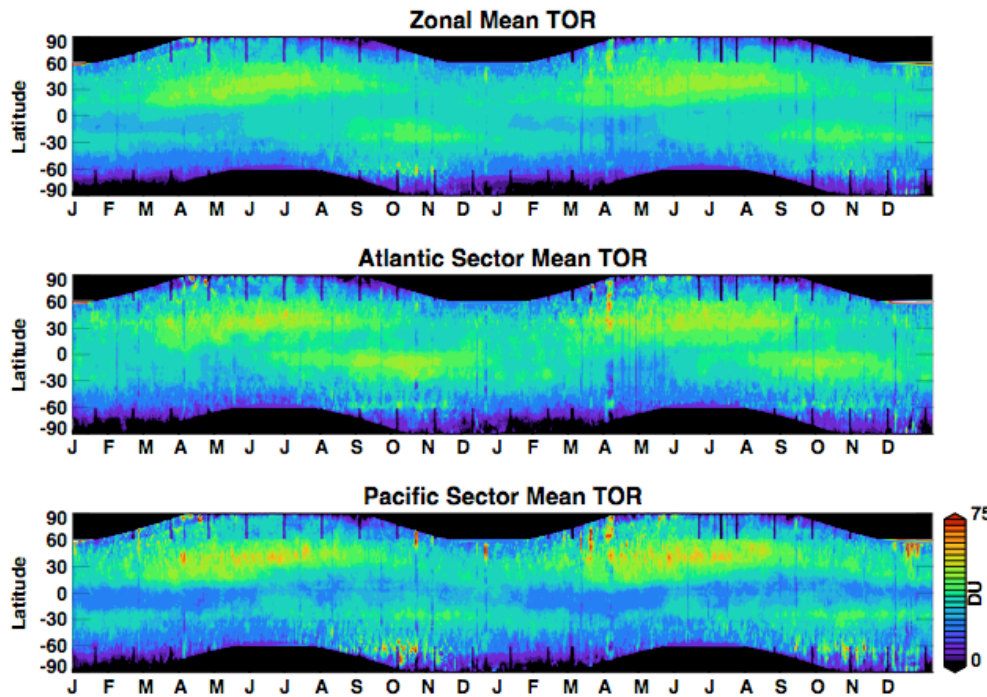


Figure 9. Zonal mean tropospheric ozone for 2005 – 2006 (top). Atlantic sector mean ozone  $75^{\circ}\text{W}$ - $15^{\circ}\text{E}$  (middle). Pacific sector mean ozone  $135^{\circ}\text{E}$  –  $120^{\circ}\text{W}$  (bottom).

Figure 9 shows the zonal mean TOR verses time for three cases, globally, the Atlantic sector ( $75^{\circ}\text{W}$ - $15^{\circ}\text{E}$ ) and the Pacific sector ( $135^{\circ}\text{E}$  –  $120^{\circ}\text{W}$ ). Once each month OMI performs a zoom

in maneuver which leaves a gap in the global data due to incomplete swaths. Between  $\pm 60^\circ$  the data shown in Fig. 9 is interpolated across the gaps.

Fig. 9 shows that the increase in TOR in the Northern Hemisphere (NH) begins in April starting at  $\sim 20^\circ\text{N}$  and moving northward. Ozone begins to decrease in August and minimizes during winter. In the Southern Hemisphere (SH), a similar increase develops in September at  $20^\circ\text{S}$  and at  $60^\circ\text{S}$ . In the tropics, the zonal mean minimum occurs from late January to June.

The mid-latitude spring NH increase likely begins with influx of ozone from the stratosphere that occurs in late winter. The build up continues through July with increases in tropospheric ozone due to pollution. In the SH a similar increase occurs at  $30^\circ$ -  $40^\circ\text{S}$ . This increase is enhanced by African and South American biomass burning which gives rise to the South Atlantic anomaly [e.g. *Edwards, et al., 2003, Thompson et al., 1996, Fishman and Larsen, 1987*] also seen in the annual mean (Fig. 8). The biomass burning enhancement shows up clearly in the contrast between the Atlantic and Pacific sectors seen in Fig. 9. In the tropics, very low ozone occurs in the Pacific sector as a result of convection and tropopause uplift.

## 5. Comparison to Z06

The TOR methods used in Z06 and this paper are not identical. Figure 10 shows April 1, 2005 for Z06 and the TTOR interpolated to the Z06 grid. Black regions in both maps indicate where the data has been flagged for quality. Overall the maps are similar except for the very high and low regions in Z06 – most of which have been flagged in the lower figure. For example, the high TOR patch over the mid-North America is flagged in the TTOR. The very low region to the just to the west is significantly lower in Z06 than this product. We have been able to show that very high and low regions paired, such as in this example, are the result of assuming that the data are synoptic when it is actually asynoptic. The asynoptic correction used in the TTOR tends to reduce the amplitude of fold events.

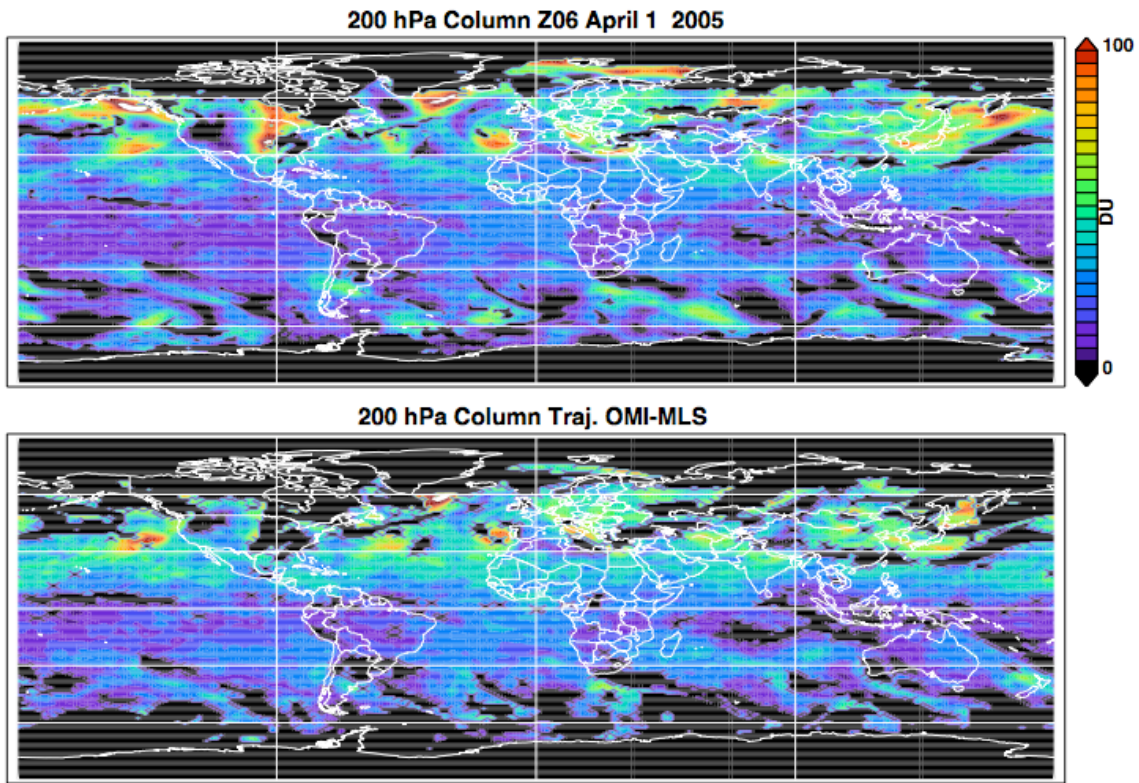


Figure 10. Upper figure, 200TSC for April 1, 2005 calculated using the algorithm in Z06. Lower figure, TTOR 200TSC interpolated to the Z06 grid. Dark areas are flagged regions meaning the results are questionable due to, for example, high reflectivity or low tropopause.

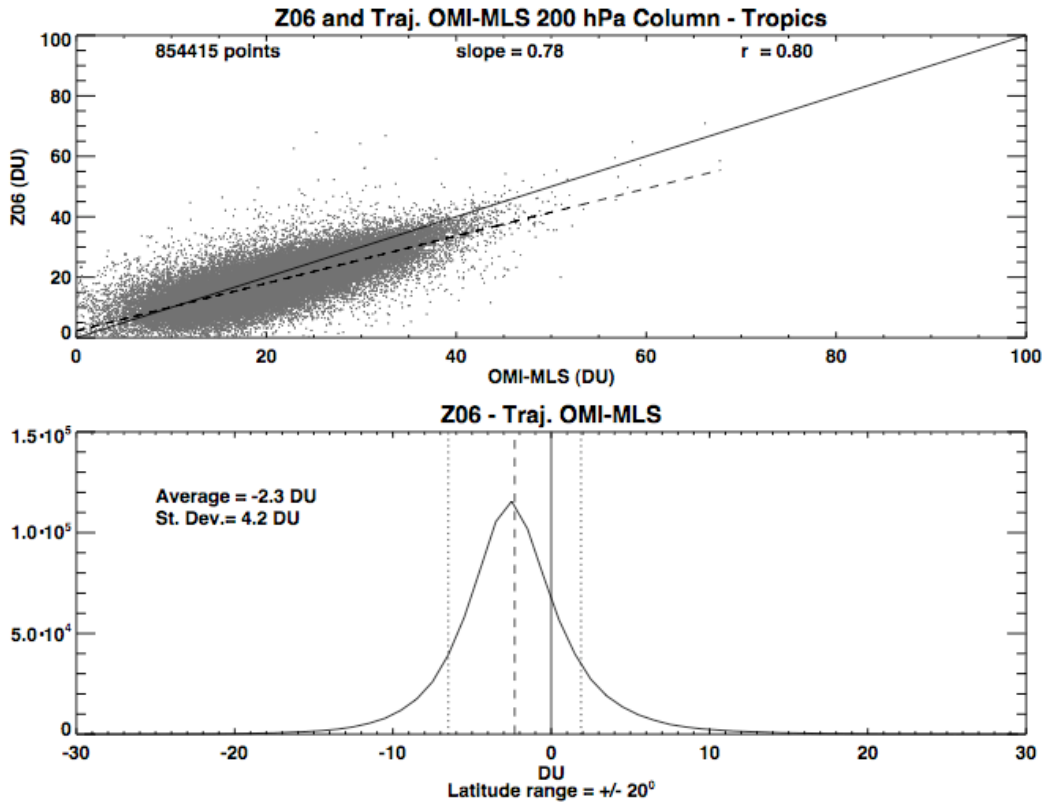


Figure 11. comparison of this OMI-MLS 200 hPa column to surface product with Z06 in the region  $\pm 20^\circ$  latitude as in Figure 3.

Figure 11 shows a tropical comparison of Z06 and TTOR. We don't expect a perfect correlation because of the different scheme for creating the high resolution stratosphere, nonetheless, the correlation is quite high. The offset of 2.3 DU is due to ozone explicitly added to the Z06 product based on recent evaluation of OMI and MLS SCO offset differences for September 2004 - December 2006 [J. Ziemke, personal communication, 2007]. The difference PDF is Gaussian with a fairly small standard deviation, ~4 DU, reflecting the overall similarity between the schemes.

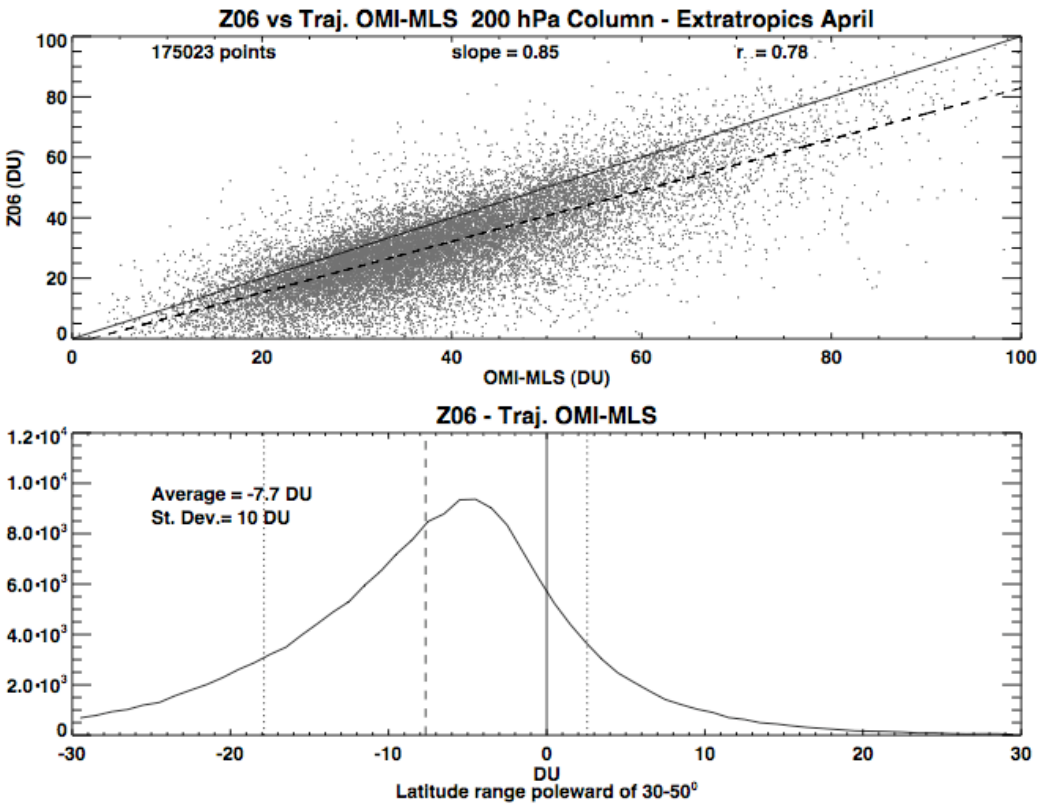


Figure 12. Comparison of the 200TSC from Z06 and this product for April 2005 as in Figure 11. Extra-tropical range is 30°N to 50°N latitude.

Figure 12 shows the mid-latitude comparison for July 2005. The correlation coefficient is high despite the higher scatter. We also see an offset of about 6.5 DU which is not entirely due to the explicit addition of ozone in Z06. Referring back to Figure 10 (which shows one day) we see that there are higher values in the Z06 product compared to this one due to the synoptic assumptions in that calculation. This creates a skewed distribution and a higher mean bias shown in the figure. Other months (not plotted here) show similar results.

## 6. Comparison with the Global Modeling Initiative Combined Stratosphere-Troposphere CTM.

Z06 describe the Global Modeling Initiative (GMI) chemical transport model. The GMI model includes both tropospheric and stratospheric chemistry. This model has been recently re-run updating the chemistry and pollution sources. The results are shown in Figure 13 and are

compared the TTOR zonal mean results from Fig. 9. Overall the GMI model agrees with the TTOR estimates; however, we note some important differences. TTOR values at high zenith angles appear to be systematically lower than GMI. The GMI model also shows slightly lower tropical tropospheric values from June through November, and slightly higher tropical values from January-March. We also see a wider band of high ozone values at subtropical latitudes in GMI than in the TTOR.

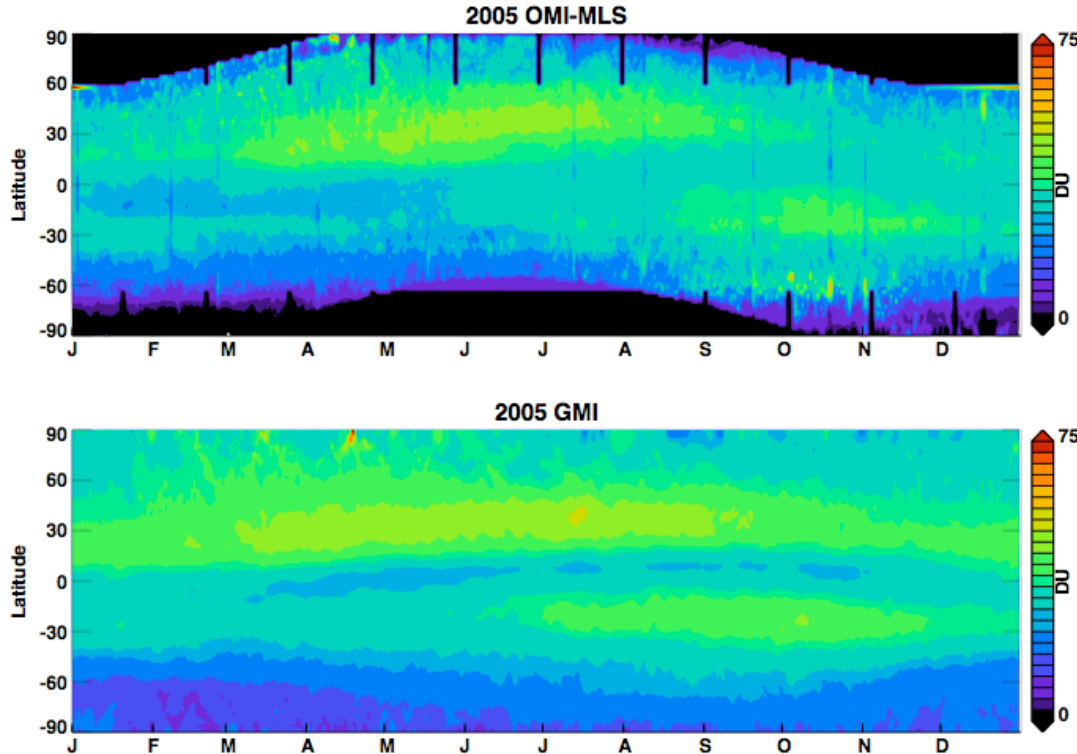


Figure 13. The zonal mean annual cycle for 2005 with this product and the zonal mean TOR shown in Figure 9.

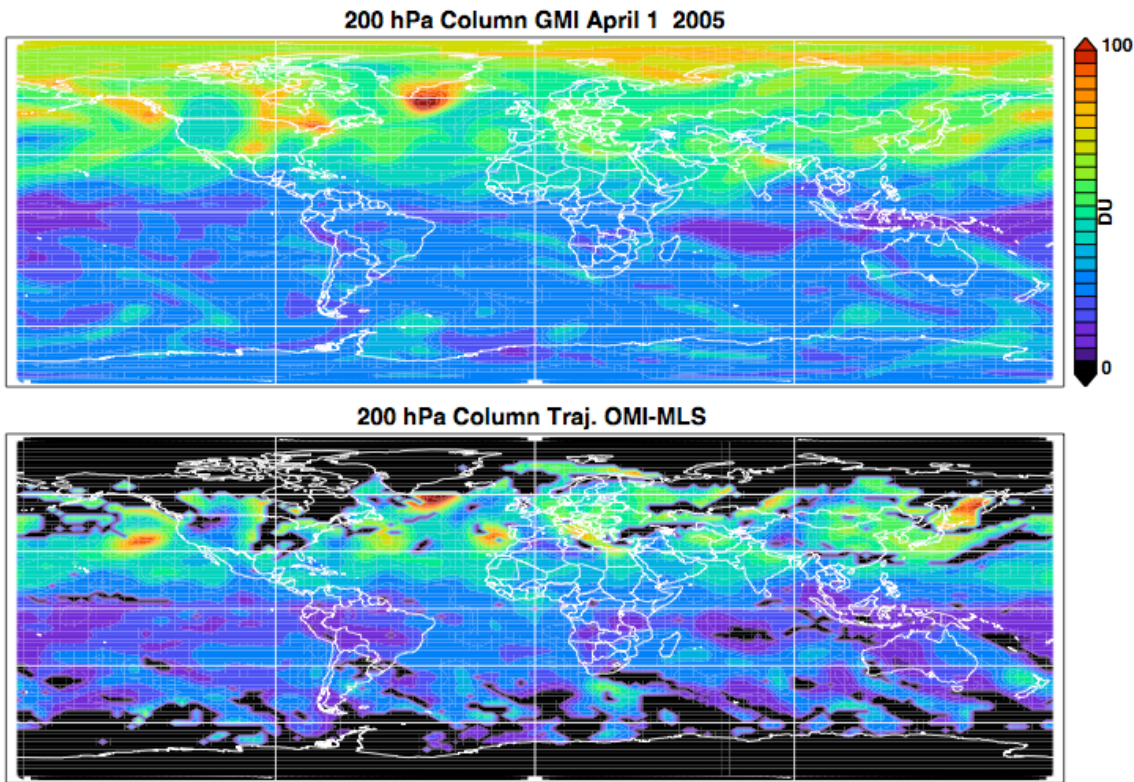


Figure 14 shows April 1 2005 GMI (top) and the TTOR 200hTSC (bottom).

Overall the GMI and the TTOR products are quite close, even some extreme features such as the high ozone field off the tip of Greenland are represented. However, there are some differences that warrant further investigation such as the high feature between Hawaii and the west coast of the United States that appears to be only weakly represented in the GMI product. We also note lower ozone amounts over South America and equatorial Africa. Figure 15 shows the difference statistics between the tropical GMI and the TTOR 200TSC for April 2005. There is a good correlation and the offset is about 2 DU; the standard deviation is about 5 DU and the statistics are Gaussian suggesting that the differences are fairly random.

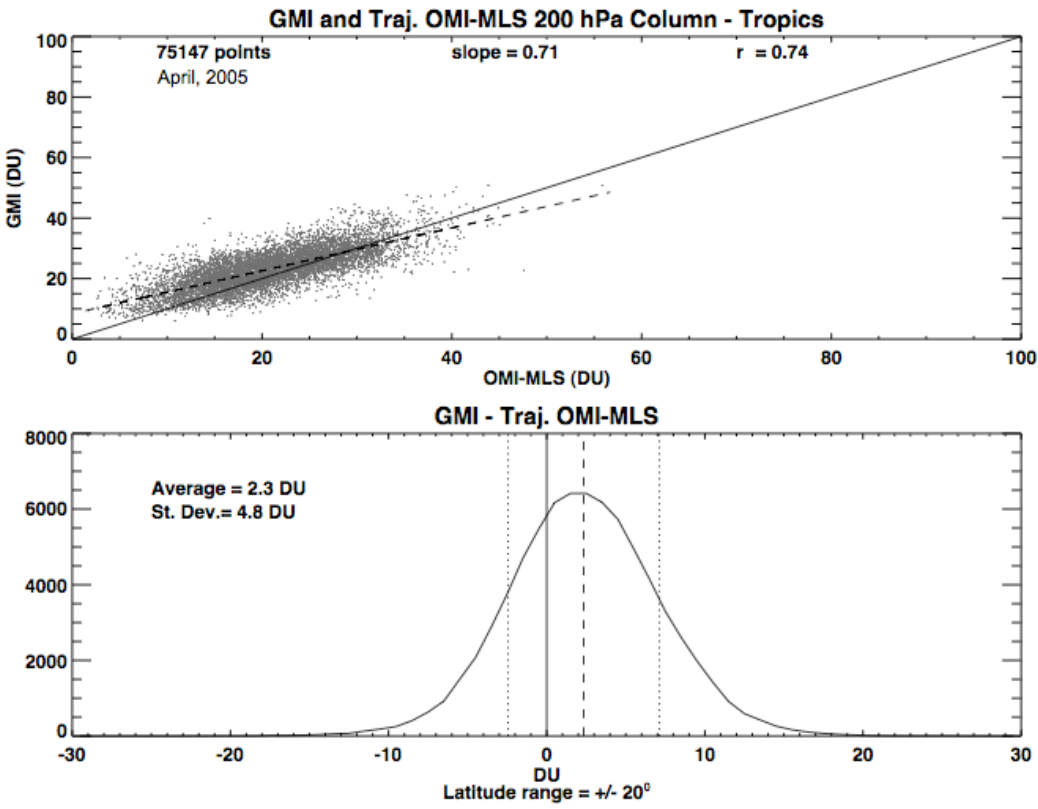


Figure 15 comparison of the TTOR and GMI 200TSC in the region  $\pm 20^\circ$  latitude as in Figure 3.

Mid-latitude comparison with GMI shows poorer agreement as seen in Fig. 16. There is poorer correlation and a wider distribution of differences. Overall, the GMI column variation has a much smaller ozone column range. This smaller range is also evident in the single day comparison shown in Fig. 14.

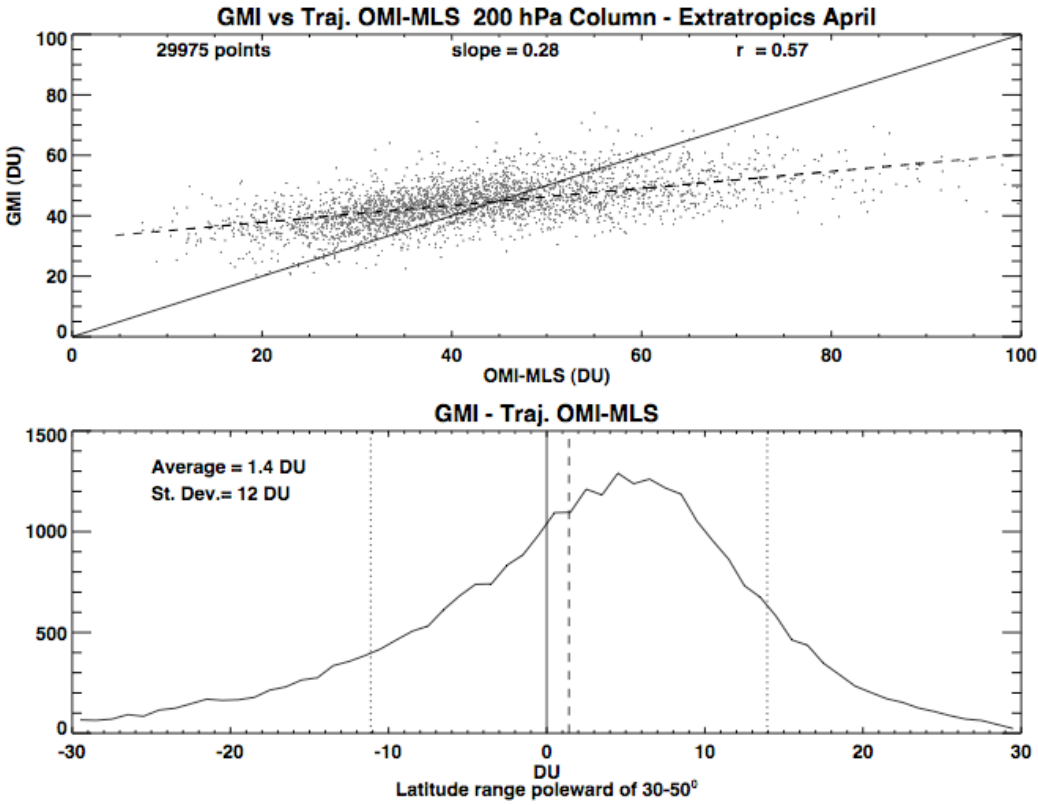


Figure 16 Northern mid-latitude comparison of GMI and the OMI-MLS surface to 200 hPa product.

## 7. Summary

Forward trajectories are used to increase the spatial resolution of the stratospheric ozone column in order to produce a higher resolution tropospheric column ozone (TCO) using the residual method. We use the OMI-TOMS algorithm for the total column and MLS V1.5 for the stratosphere. We refer to this product as the Trajectory Total Ozone Residual (TTOR). We compare the 200hPa- to-surface column (200TSC) TTOR against the 200TSC from sondes and TES measurements. Using the 200TSC removes issues associated with different tropopause definitions. Comparisons with sondes and TES show good agreement in the tropics and reasonable agreement at middle latitudes. However there is a persistent low bias in the TTOR which appears to be due to high bias in the MLS (V1.5) lower stratospheric mixing ratio. This low bias led Z06 to add 2.3DU of ozone to their product which shows up in our comparisons with their product. We also note that there is much more variability in the mid-latitude TTOR

than ozonesondes show. We speculate that this is due to the inability of MLS to resolve the steep ozone gradient at the mid-latitude tropopause.

There is a strong correlation of extra-tropical TCO anomalies with probable troposphere-stratosphere folds that are identified by large tropopause height gradients. TOR anomalies due to folds may be mistaken for pollution events since they often occur in the Atlantic and Pacific pollution corridors. We also compare the 200TSC with GMI estimates of the tropospheric column. While the tropical comparisons are good, we note that GMI variations in 200TSC at middle latitudes are much smaller than those estimated using TTOR thus GMI is somewhat closer to the ozonesondes analysis; however, more extensive comparisons between GMI and ozonesondes remain to be done.

**Acknowledgments.** Ozonesonde data obtained through the NASA Aura Validation Data Center and contributions from the ESA Envisat Cal/Val data center and the WMO GAW regional collection center for ozonesondes (NILU, Norway). The Dutch-Finnish built OMI instrument is part of the NASA EOS Aura satellite payload. The OMI Project is managed by NIVR and KNMI in the Netherlands. Funding for this research was provided by NASA's Earth Science Mission.

## References.

- Beer, R., TES on the Aura mission: Scientific objectives, measurements and analysis overview, *IEEE Trans. Geosci. Remote Sensing*, 1102-1105 , 2006.
- Bhartia, P. K., Total ozone from backscattered ultraviolet measurements, in *Observing Systems for Atmospheric Composition*, pgs 48-63, Springer Science, New York, 2007.
- Bloom, S., et al., Documentation and validation of the Goddard Earth Observing System (GEOS) Data Assimilation System – Version 4, *Technical Report Series on Global Modeling and Data Assimilation* 104606, 2005.
- Chandra, S., J. R. Ziemke, and R. V. Martin, Tropospheric ozone at tropical and middle latitudes derived from TOMS/MLS residual: Comparison with a global model, *J. Geophys. Res.*, 108(D9) doi:10.1029/2002JD002912, 2003.
- Dessler, A., *The Chemistry and Physics of the Stratosphere*, Elsevier Limited, 214 pp, 2005.

de Laat, A. T. J., I. Aben, and G. J. Roelofs, A model perspective on total tropospheric O<sub>3</sub> column variability and implications for satellite observations, *J. Geophys. Res.*, 110, D13303, doi:10.1029/2004JD005264, 2005.

Edwards, D. P., et. al., Tropospheric ozone over the tropical Atlantic: A satellite perspective, *J. Geophys. Res.*, doi:10.1029/2002JD002927, 2003.

Fishman, J., and J. C. Larsen, Distribution of total ozone and stratospheric ozone in the tropics: Implications for the distribution of tropospheric ozone, *J. Geophys. Res.*, 92, 6627-6634, 1987.

Fishman, J., C. E. Watson, J. C. Larsen, and J. A. Logan, Distribution of tropospheric ozone determined from satellite data, *J. Geophys. Res.*, 95(D4), 3599-3617, 1990.

Froidevaux, L. et al., Validation of Aura Microwave Limb Sounder stratospheric ozone measurements, *J. Geophys. Res.*, *this issue*, 2007.

Froidevaux, L. et al., Early validation analyses of atmospheric profiles from EOS MLS on the Aura satellite, *IEEE Trans. Geosci. Remote Sensing*, 1006-1121, 2006.

Kulawik, S.S., J. Worden, A. Eldering, K. Bowman, M. Gunson, G.B. Osterman, L. Zhang, S.A. Clough, M.W. Shephard, and R. Beer, Implementation of cloud retrievals for Tropospheric Emission Spectrometer (TES) atmospheric retrievals: part 1. Description and characterization of errors on trace gas retrievals, *Journal of Geophysical Research-Atmospheres*, 111 (D24), 2006.

Kley, D., et al., Observations of near-zero ozone concentrations over the convective Pacific: Effects on air chemistry, *Science*, 274, 230-232, 1996.

Lelieveld, J., et al., Global air pollution crossroads over the Mediterranean, *Science*, 298(5594), 794-799, 2002.

Levelt, P. F., et al., The Ozone Monitoring Instrument, *IEEE Trans. Geophys. Rem. Sens.*, 44, 1093-1101, 2006.

Liu, X., et al., Ozone profile and tropospheric ozone retrievals from the Global Ozone Monitoring Experiment: Algorithm description and validation, *J. Geophys. Res.*, 110, D20307, doi:10.1029/2005JD006240, 2005.

Liu, X., et al., First directly-retrieved global distribution of tropospheric column ozone from GOME: Comparison with the GEOS-CHEM model, *J. Geophys. Res.*, 111, D02308, doi:10.1029/2005JD006564, 2006.

Livesey, N. et al., Validation of Aura Microwave Limb Sounder O<sub>3</sub> and CO observations in the upper troposphere and lower stratosphere, *J. Geophys. Issue. (this issue)*, 2007.

- Martin, R. V., et al., Interpretation of TOMS observations of tropical tropospheric ozone with a global model and in situ observations, *J. Geophys. Res.*, 107, 10.1029/2001JD001480, 2002.
- Marufu, L., et al., Photochemistry of the African troposphere: Influence of biomass burning emission, *J. Geophys. Res.*, 105, 14,513-14,530, 2000.
- Morris, G.A., J. F. Gleason, J. Ziemke and M. R. Schoeberl, Trajectory mapping: A tool for validation of trace gas observations, *J. GEOPHYSICAL RES.* 105 (D14): 17875-17894 2000.
- McPeters, R.D., et al., Validation of the total column ozone data product of the Ozone Monitoring Instrument aboard NASA EOS-Aura, *J. Geophys. Res.* this issue, 2007.
- Morris, G. A. et al., Trajectory Mapping And Applications To Data From The Upper-Atmosphere Research Satellite, *J. Geophys. Res.* 100, 16491-16505, 1995.
- Moxim, W. J., and H. Levy II, A model analysis of tropical South Atlantic Ocean tropospheric ozone maximum: The interaction of transport and chemistry, *J. Geophys. Res.*, 105, 17,393-17,415, 2000.
- Osterman, G.B. et al., Validation of Tropospheric Emission Spectrometer (TES) Measurements of Total Column and Stratospheric Ozone, *J. Geophys. Res.*, this issue., 2007.
- Randel, W. J., D.J. Seidel, and L.L. Pan, Observational characteristics of double tropopauses, *Journal of Geophysical Research*, 112, D07309, doi:10.1029/2006JD007904, 2007.
- Schoeberl, M. and L. C. Sparling, Trajectory Modeling, Diagnostic Tools in Atmospheric Science, Proceedings of the International School of Physics, Enrico Fermi, G. Visconti, ed., 289-305, 1995.
- Schoeberl, M. R. Extra tropical stratosphere-troposphere mass exchange, *J. Geophys. Res.*, 109, D13303, 2004.
- Schoeberl, M. R., et al., Overview of the EOS Aura Mission, *IEEE Transactions on Geosci. and Remote Sensing*, 44, 1066-1074, 2006.
- Stajner, I. et al., Assimilated ozone from EOS-Aura: Evaluation of the tropopause region and tropospheric columns, *J. Geophys. Res.*, this issue, 2007.
- A. M. Thompson, K. E. Pickering, D. P. McNamara, M. R. Schoeberl, R. D. Hudson, J. H. Kim, E. V. Browell, V. W. J. H. Kirchhoff, and D. Nganga, Where did tropospheric ozone over southern Africa and the tropical Atlantic come from in October 1992? Insights from TOMS, GTE/TRACE-A and SAFARI-92, *J. Geophys. Res.*, 101, 24,251-24,278, 1996.
- Thompson, A. M., et al., Southern Hemisphere Additional Ozonesondes (SHADOZ) 1998-2000 tropical ozone climatology: 1. Comparisons with Total Ozone Mapping Spectrometer

(TOMS) and ground-based measurements, J. Geophys. Res., 108(D2), 8238, doi:10.1029/2001JD000967, 2003.

Thompson, A. M., et al., IONS (INTEX Ozonesonde Network Study, 2004): 1. Summertime UT/LS (Upper Troposphere/Lower Stratosphere) Ozone over Northeastern North America, J. Geophys. Res., 112, doi: 10.1029/2006JD007441, in press, 2007.

Waters, J. W., et al., The Earth Observing System Microwave Limb Sounder (EOS MLS) on the Aura satellite, *IEEE Trans. Geosci. Remote Sensing*, 1075-1092 , 2006.

Worden, H. M., et al. , Comparisons of Tropospheric Emission Spectrometer (TES) ozone profiles to ozonesodes: methods and initial results, J. Geophys. Res., 112, D03309, doi:10.1029/2006JD007258, 2007.

Ziemke, J. R., et al., Tropospheric ozone determined from aura OMI and MLS: Evaluation of measurements and comparison with the Global Modeling Initiative's Chemical Transport Model, J. Geophys. Res., 111, D19303, doi: 10.1029/2006JD007089, 2006.